

Experimental evidence for quantum-size-effect fine structures in the resistivity of ultrathin Pb and Pb-In films

M. Jałochowski

Institute of Physics, Maria Curie-Skłodowska University, Pl. M. Curie-Skłodowskiej 1, PL-20-031 Lublin, Poland

E. Bauer, H. Knoppe, and G. Lilienkamp

Physikalisches Institut, Technische Universität, Clausthal, D-3392 Clausthal-Zellerfeld, Federal Republic of Germany

(Received 26 December 1991)

The resistivity of ultrathin single-crystalline Pb and Pb-In layers with thicknesses d smaller than the bulk mean free path l , is measured during deposition onto Si(111)-(6×6)Au surfaces at about 110 K. The structure of the layers is monitored by reflection high-energy electron diffraction (RHEED). Oscillations of the RHEED specular beam intensity are highly correlated with fine structures of the resistivity. The quantum-size-effect theory is used for a quantitative analysis of the data. The fine structure, volume impurities, small-scale roughness, and large-scale thickness fluctuations are taken into account. The impact of the layer-by-layer growth mode of ultrathin metal films on the thickness dependence of the resistivity is discussed.

I. INTRODUCTION

A large number of investigations of the electrical conductivity of thin metal films have been published. The results are usually analyzed in terms of the Fuchs-Sondheimer theory¹ and its extensions.² These theories are based on the Boltzmann equation. The film is characterized by the resistivity ρ_∞ of the bulk metal and the mean free path l . Surface effects are incorporated via the specularity parameter p which is the fraction of the conduction electrons specularly reflected from the surfaces. This classical size-effect theory (CSE) breaks down in films with thickness $d < l$ and when the energy-level spectrum is discrete. In these situations a quantum-mechanical treatment of the problem is required.

Quantum-size effects (QSE) in films with perfect surfaces were studied theoretically by Sandomirski,³ who solved the Boltzmann transport equation with a δ -function potential for randomly distributed static impurities. He obtained an oscillatory dependence of the electrical resistivity of semimetallic thin films upon thickness with an oscillation period of one-half of the Fermi wave length λ_F . Using the Kubo formalism,⁴ Govindaray and Devanathan⁵ have calculated the resistivity of thin aluminum and copper films. Their result was in good agreement with the result of Sandomirski.

The influence of surface roughness on the conductivity of size-quantized thin metal films was studied by Leung.⁶ He introduced the autocorrelation function of the rough surface profile and pointed out the importance of surface scattering in the description of the electron transport in ultrathin metal films. Tešanović and Jarić⁷ discussed the effect of surface scattering on quantum transport in thin films with uncorrelated atomically rough surfaces. Their results were applied to CoSi₂ (Ref. 8) to explain the enhancement of the resistivity for very thin films.

More recently Trivedi and Ashcroft⁹ thoroughly discussed the influence of random surface roughness on the QSE. In their work surface roughness is incorporated as a boundary condition on the Hamiltonian, and for sufficiently small variation of the thickness the problem is handled perturbatively. They also included large-scale thickness fluctuations on a scale larger than the mean free path by breaking up the film into units with slightly different thicknesses. Using the particle-in-box model they found results essentially similar to Sandomirski's but strongly modified in the ultrathin film range if small-scale surface roughness was included.

Most recently the influence of surface roughness correlations on the surface conductivity of thin films was studied theoretically by Fishman and Calecki.¹⁰ For small roughness correlation lengths ξ , in the limit $\xi k_l \ll 1$ where k_l is the largest of the Fermi wave vectors k_ν of subband ν , they found the dependence $\sigma \propto d^\alpha$ with α decreasing from 6 when the number of occupied subbands N is 1, to $\alpha=2.1$ when $N \gg 1$. On the other hand, for $\xi k_l > 1$, α becomes smaller than 2.3. These α values differ considerably from the classical value $\alpha=1$.

Although the occurrence of quantum-size effects in the resistivity has been reported,^{11,12} there is still controversy about the influence of the real structure of the thin film on its resistivity. It is obvious that the thickness of the crystalline film cannot be varied infinitesimally and from that it follows that in the free-electron model the QSE condition is fulfilled when $nd_0 = m\lambda_F/2$, where n and m are integers, d_0 is the monolayer thickness, and λ_F is the Fermi wave length. Experimental evidence of this phenomenon was previously reported in Ref. 13, in which the resistivity of ultrathin epitaxial Pb layers was measured and simultaneously reflection high energy electron diffraction (RHEED) specular beam intensity oscillations with 1-ML (monolayer) period were seen. This supports the idea that during monolayer-by-monolayer growth the

surface roughness of the film is changing periodically with thickness, which also influences the resistivity of the film. The purpose of this paper is to provide further evidence of the influence of surface roughness by a more detailed analysis of additional studies of Pb and Pb-In films.

It has been shown previously that the growth mode of Pb on the Si(111) surface can be modified by evaporation of other elements. About 0.5 at. % of Ag remarkably prolonged the layer-by-layer growth mode.¹⁴ The same was true for Au codeposition at the same rate. Similarly, by coevaporation of In and Pb we were able to modify the surface roughness of the growing film. This allowed us to vary the size-effect fine structures in the electrical resistivity. In was chosen because of its complete miscibility with Pb and its similar surface energy so that no phase separation or surface segregation has to be expected.

The paper is organized as follows: In Sec. II the experimental details are discussed. The results of the RHEED specular beam intensity measurements are presented in Sec. III A. Experimental resistivity data and a discussion of the CSE parameters in Pb and Pb-In are given in Sec. III B. In Sec. III C the resistivity fine structures are analyzed in the framework of the quantum theory given in Ref. 9 and the role of surface roughness is discussed. A simple growth model¹⁵ is adapted and finally the electrical conductivity of ultrathin films is calculated and compared with experimental data. Quantitative agreement is obtained using parameters of thicker Pb films. Section IV contains an analysis and discussion of the results. We show that the CSE fine structure can be properly described by the QSE theory after introducing a simple monolayer-by-monolayer growth model.

II. EXPERIMENT

The experiments were performed in a UHV molecular-beam epitaxy system equipped with various electron- and photon-induced electron spectroscopies. The system was pumped by a titanium sublimation pump and by an LN₂-baffled diffusion pump which produced a base pressure of 4×10^{-9} Pa and maintained a pressure below 1×10^{-8} Pa during deposition. Pb and In were evaporated from Mo crucibles and Au from a W crucible by electron-bombardment heating.

The substrates were Si(111) single crystals with 1000 Ω cm resistivity at room temperature, cut with an accuracy of $\pm 0.05^\circ$ and typical dimensions $16 \times 4 \times 0.8$ mm³. They were polished, etched in 19:1 HNO₃+HF solution, rinsed in distilled water and methanol, and mounted in a Mo holder. The final surface cleaning consisted in flashing for a few seconds to about 1500 K. This treatment produced a sharp (7 \times 7) superstructure RHEED pattern. Direct resistive heating of the Si crystal was used. The holder could be rotated so that any polar angle could be selected for the RHEED intensity measurements. The substrate could be cooled to about 110 K by cooling the crystal holder with LN₂.

The thickness of the growing films was measured with a quartz-crystal oscillator. In order to modify the surface of Si chemically and structurally about 1.2 ML Au was deposited. The Au deposits were annealed for 1 min at

about 950 K and then the temperature was gradually lowered to about 500 K within 3 min. This resulted in the appearance of the (6 \times 6)Au superstructure which altered the growth mode of Pb on Si(111) and changed the interfacial parameters in the Si(111)/Pb system.^{13,14}

RHEED intensity measurements were made with a home-built magnetically focused high-resolution RHEED gun equipped with several deflection systems for beam alignment. A Faraday cup detector could be moved into any desired position in the central part of the RHEED pattern which was simultaneously observed on the fluorescent screen. All measurements reported below were taken with 20-keV electrons under specular conditions.

The electrical resistivity was measured as follows. The 140-Hz signal from a signal generator was applied to the sample in series with a 5-M Ω resistor. The substrate with the Au(6 \times 6) superstructure had typically 10–20 k Ω resistance at 110 K. A signal which was proportional to $R_{\parallel} = R_s R_f / (R_s + R_f)$, where R_s is the resistance of the substrate and R_f that of the film, was obtained from potential contacts consisting of electrochemically etched W wires pressed against the front of the Si crystal. Careful calibration of the electronics and collection of the data by a computer allowed a broad dynamical range and a high accuracy of the measurements.

III. RESULTS AND DATA ANALYSIS

A. RHEED specular beam intensity oscillations

It is well established that the occurrence of the RHEED intensity oscillations indicates quasi-monolayer-by-monolayer growth. This phenomenon has been observed in semiconductors,¹⁶ and subsequently also during the growth of ultrathin metal films.^{17,18} We have observed RHEED specular-beam intensity oscillations in ultrathin films of Pb and Pb-In alloys during their growth on Si(111)-(6 \times 6)Au substrates at about 110 K. Figure 1 shows typical results of RHEED intensity oscillation measurements for thin films evaporated on Si(111)-(6 \times 6)Au at 110 K. For the pure-Pb film the oscillations are regular from the very beginning and are strongly damped. The additional structure in the initial stage of growth is presumably caused by the interaction of the beam with the substrate and can be explained only within the framework of the dynamical theory of diffraction. Also, a possible QSE in RHEED intensity oscillations has to be taken into account.¹³ With increasing In content the RHEED intensity oscillations extended up to increasingly larger thickness (Fig. 1). At around 30 at. % of In they were best developed. For these samples the oscillations become regular, however, only after deposition of about four monoatomic layers of Pb-In as indicated by the RHEED pattern. A similar transition from disordered to well-ordered thin film was previously reported¹⁴ for pure Pb on Si(111)-(7 \times 7), where the RHEED intensity started to oscillate regularly after reaching a critical thickness of about 4 ML.

The thickness of the Pb-In alloy monolayer at 110 K

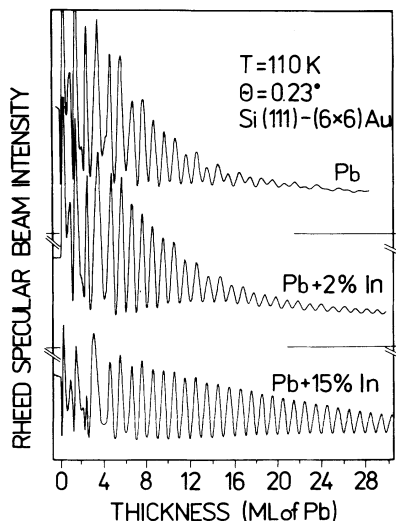


FIG. 1. RHEED specular beam intensity oscillations during growth of Pb and Pb-In films on a Si(111)-(6×6)Au surface at 110 K. [112] azimuth, glancing angle $\Theta=0.23^\circ$.

was determined by RHEED intensity oscillation and the oscillator measurements. It was found to be constant up to 30 at. % of In, within accuracy of $\pm 1\%$. This is consistent with the crystal structure data for the Pb-In system.¹⁹ Up to 73 at. % In only one phase with fcc crystal structure exists whose lattice constant varies from 4.94 Å for pure Pb to 4.81 Å for Pb-In with 73 at. % of In.

B. Resistivity of ultrathin Pb and Pb-In films

As examples for all evaporated samples we select for further discussion three samples with very different contents of In, 0, 6, and 25 at. % for samples *A*, *B*, and *C*, respectively. The thickness dependence of the specific conductivity as calculated from the experimental data is shown in Fig. 2. Similar to our earlier investigations¹³ the experimental data could be fitted by the Sondheimer approximation to the Fuchs formula for $d/l > 1$, with d the thickness, l the mean free path, as follows:

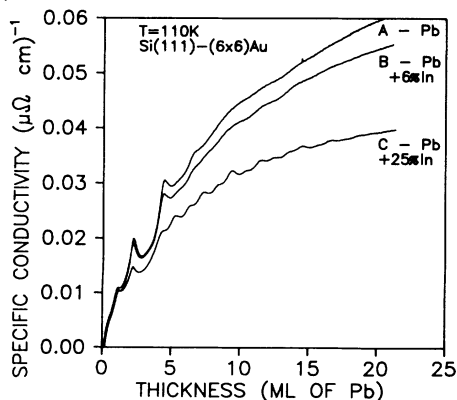


FIG. 2. Specific conductivity vs thickness of films of Pb with 0, 6, and 25 at. % of In measured at 110 K.

TABLE I. Pb film parameters derived from the experimental data of Fig. 2 using Eq. (1).

Sample type	at. % of In	ρ_∞ ($\mu\Omega$ cm)	$(1-p)l$ (Å)
<i>A</i>	0	11.6	71.8
<i>B</i>	6	12.8	68.9
<i>C</i>	25	19.1	49.1

$$\rho(d) = \rho_\infty [1 + 3l(1-p)/8d] . \quad (1)$$

p is the specularity parameter. The specific resistivity of the bulk material ρ_∞ and the parameter $l(1-p)$ were obtained from a least-squares fit within the thickness range in which the fine structure in the resistivity is weak. This range began typically at about 15 Å. The data for the examples are shown in Table I.

We are now able to find the ρ_s vs d dependence, where ρ_s is the surface residual resistivity $\rho_s = \rho(d) - \rho_\infty$. This is shown in the $\log_{10}(\rho_s)$ vs $\log_{10}(d)$ plots of Fig. 3. In the oscillation-free regions of the curves the slope α of the $\sigma_s \propto d^\alpha$ dependence was 1, with an accuracy of 3% ($\sigma_s = 1/\rho_s$). Also the data for extremely thin films (from 1 to about 10 Å) follow the linear dependence with a superposed modulation caused by QSE and CSE contributions. In this sense the data are very well described by the classical formula (1), although the applicability of such a description is rather questionable.

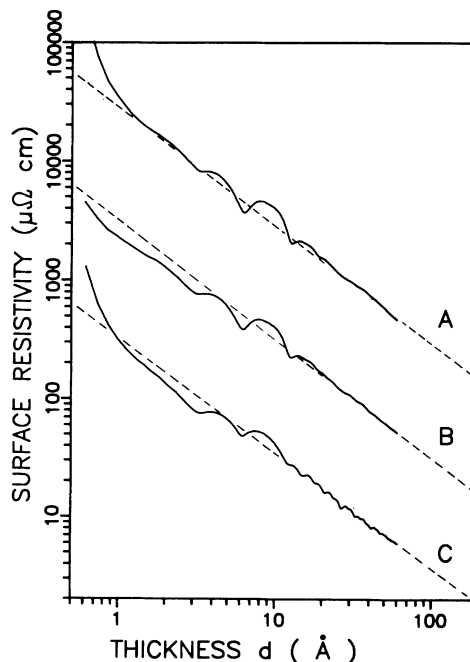


FIG. 3. $\log_{10}(\rho_s)$ vs $\log_{10}(d)$ plot. ρ_s was obtained by subtraction of ρ_∞ from the data of Fig. 2. The dashed lines show the dependence $\sigma \propto d$. The data of curves *B* and *A* are multiplied in the plot by 10 and 100, respectively.

C. Fine structures in the resistivity

The modulation of the smooth $\sigma_s \propto d$ dependence seen in the data of Fig. 3 can have two causes: the CSE and the QSE. The CSE is introduced by the periodic variation of the parameter p in Eq. (1). This oscillation is strongly linked with the RHEED intensity oscillations and originates from the periodic change of the surface roughness induced by the quasi-monolayer-by-monolayer growth as discussed previously.^{13,14} It is expected that the period of the resistivity oscillations corresponds to that of the RHEED intensity oscillations and is equal to 1 ML. This was found to be true for all samples. Codeposition of In enhances this effect strongly, as clearly seen in the RHEED and resistivity data.

Figure 4 shows the data for the samples *A*, *B*, and *C* obtained after subtraction of $1/\rho(d)$ calculated according to Eq. (1) with the parameters of Table I, from the measured data. The amplitude of the 1-ML oscillation period increases with increasing In concentration. Superimposed on it is a 2-ML oscillation period. The 1-ML fine structure in the electrical resistivity of ultrathin metal films as a pure classical size effect was previously reported in Au (Ref. 20) deposited at 100 K on Si(111)-(7×7). The 2-ML-period oscillation can be explained by the QSE. A QSE in the resistivity for (111) epitaxy of Au is excluded by the band structure of Au because of the energy gap in the ΓL branch near the Fermi level.²¹ In Pb-In alloys a QSE is possible. The 1-ML-periodicity fine structure in the electrical resistivity of the Pb-In films may be used as a reference to determine precisely the QSE structures in the $\sigma(d)$ plots.

The analysis of the QSE is made according to the theory described in Ref. 9. In the presence of bulk impurity scattering and surface roughness scattering the conductivity in the plane of thin film is

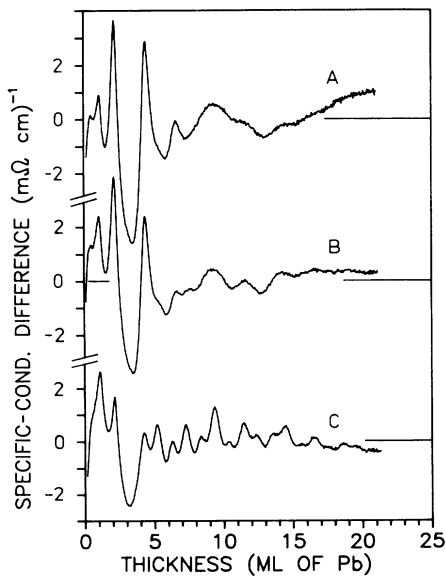


FIG. 4. Specific conductivity difference $\sigma_d = 1/\rho_{\text{exp}} - 1/\rho(d)$. $\rho(d)$ is calculated according to Eq. (1) with the parameters of Table I. $1/\rho_{\text{exp}}$ are the data of Fig. 2.

$$\sigma_{xx} = \frac{e^2 k_F}{\hbar \pi^2} \frac{1}{\kappa} \sum_{n=1}^{n_c} \frac{1 - n^2/\kappa^2}{\frac{2n_c + 1}{k_F l \kappa} + \left[\frac{\delta d}{d} \right]^2 \frac{s(n_c) n^2}{3\kappa}}, \quad (2)$$

where k_F is the Fermi wave vector, $\kappa = k_F d / \pi$, $n_c = \text{Int}(\kappa)$, $s(n_c) = (2n_c + 1)(n_c + 1)n_c / (3\kappa^3)$, and l is the mean free path. δd describes the small-scale roughness and is the root-mean-square deviation of the mean film thickness d . The effect of fluctuations in the thickness of the film on a scale larger than the mean free path may be also included.⁹ The small-scale surface roughness δd is obtained from a comparison between the RHEED intensity oscillations and a growth model.¹⁵

The “distributed growth model”¹⁵ takes into account the lateral structure of the surface of a film by distributing adatoms among the monolayers according to the number of “reactive” sites available. Of the $(\Theta_n - \Theta_{n+1})/\tau$ atoms arriving per unit time on top of the n th layer, a fraction α_n transfers to the n th layer and a fraction $1 - \alpha_n$ remains on top of the n th layer. Here Θ_n is the layer coverage of the n th level and $1/\tau$ is the deposition rate. In this model the time-dependent coverage is given by the equation

$$\frac{d\Theta_n}{dt} = \alpha_n \frac{\Theta_n - \Theta_{n+1}}{\tau} + (1 - \alpha_{n-1}) \frac{\Theta_{n-1} - \Theta_n}{\tau} \quad (3)$$

and

$$\alpha_n = A \frac{d_n(\Theta_n)}{d_n(\Theta_n) + d_{n+1}(\Theta_{n+1})}. \quad (4)$$

A is the phenomenological parameter that measures the net rate of transfer from one layer to the next and d_n is an effective perimeter for the capture of an adatom to a given layer. We choose the dependence $d_n(\Theta_n) = \Theta_n(1 - \Theta_n)^{1/2}$, which corresponds to a growth model in which both the number and the size of the nucleation sites change during film growth.¹⁵ The coverage Θ_n at time t is given by the solution of the set of coupled differential equations (3) subject to the initial conditions $\Theta_0(t) = 1$, $\Theta_n(0) = 0$ for $n \geq 1$, and $\Theta_\infty = 0$.

In the anti-Bragg condition the specular electron beam intensity I in the kinematic theory of diffraction is given by¹⁵

$$I = \left[\sum_{n=0}^{\infty} (\Theta_n - \Theta_{n+1}) \cos(n\pi) \right]^2 \quad (5)$$

and the surface roughness is given by²²

$$(\delta d)^2 = \sum_{n=0}^{\infty} (n - t/\tau)^2 (\Theta_n - \Theta_{n+1}). \quad (6)$$

Solutions of Eqs. (3), (5), and (6) with $A = 0.925$ and 0.875 are shown in Fig. 5. With further decreasing value of A the RHEED intensity oscillations are strongly damped and $(\delta d)^2$ approaches the $(\delta d)^2 = t/\tau$ dependence characteristic of the nondiffusive growth model.¹⁵

Next we consider the influence of large-scale thickness fluctuations. As is evident from the $\Theta_n(t)$ definition, the mean thickness of the film d in units of ML is given by the equation

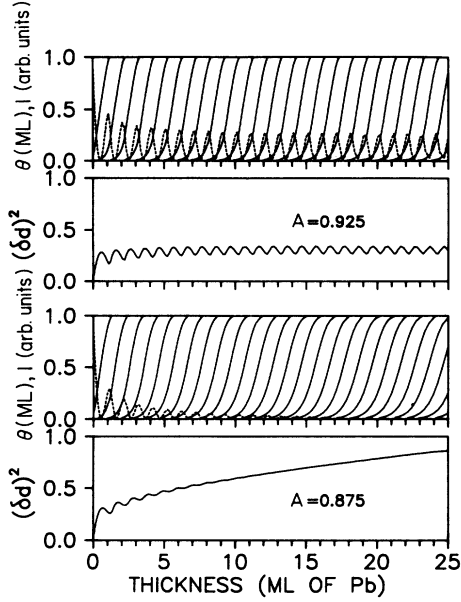


FIG. 5. Solutions of Eqs. (4) and (5) with $A = 0.875$ (bottom pair of figures) and with $A = 0.925$ (upper pair of figures). The coverage Θ (solid), the specular electron beam intensity I (dashed) calculated with Eq. (5), and the rms surface roughness $(\delta d)^2$ [in (ML)² units] calculated with Eq. (6) are shown for both values of A .

$$d(t) = \sum_{n=1}^{\infty} \Theta_n(t) d_0, \quad (7)$$

where $d(t)$ is the film thickness measured with a quartz crystal oscillator. The number of monoatomic layers with $0 < \Theta_n < 1$ depends on the thickness of the film and on the growth mode. In the early stages of the film growth only 2 ML are involved (2-ML growth front) whereas for a film 25 ML thick with $A = 0.875$ (Fig. 5), 4 monoatomic layers are partially filled (4-ML growth front). In such a film-growth mode—which occurs during the growth of all epitaxial or textured films—the sample consists of regions with thicknesses given by integer numbers of monoatomic layers [Eq. (7)] and can microscopically not be described by a mean thickness d . This fact is extremely important for the study of the QSE in thin metallic films in which λ_F is of the order of d_0 . The quantity Θ_n in the distributed growth model gives only the fraction of the total area of the sample with thickness nd_0 but does not describe the size, shape, and lateral distribution of the islands on the surface of the film. For the sake of simplicity we consider only two simple distribution models.

In the first model the sample is composed of ribbons with different thickness nd_0 aligned parallel to the direction of the current flow (x) during the resistivity measurements. The number of the ribbons is equal to the number of monolayers involved in the evolution of the growth front. Each ribbon has a width of $(\Theta_n - \Theta_{n+1})$ of the total length of the sample. The resulting average conductivity $\bar{\sigma}_p$ is given by

$$\bar{\sigma}_p = \frac{1}{d} \sum_{n=1}^{\infty} \sigma_{xx}(nd_0) (\Theta_n - \Theta_{n+1}) nd_0, \quad (8)$$

where $\sigma_{xx}(nd_0)$ is given by Eq. (2), Θ_n is obtained by the solution of Eq. (3), nd_0 is the thickness of the ribbon, and d is the average thickness of the sample.

In the second model the ribbons are aligned perpendicular to the x direction. Each ribbon with the same area as in the first model has the length $(\Theta_n - \Theta_{n+1})$ of the total length of the sample. For the average conductivity $\bar{\sigma}_s$, we get

$$\bar{\sigma}_s = \frac{1}{d} \frac{1}{\sum_{n=1}^{\infty} \frac{\Theta_n - \Theta_{n+1}}{\sigma_{xx}(nd_0) nd_0}}. \quad (9)$$

In a real sample we have to consider a net of units with different sizes and different shapes connected in a mixed form. Thus the true value of σ can be expected to lie between the limits $\bar{\sigma}_p$ and $\bar{\sigma}_s$. In fact both models give very similar results that differ less than 2% already for a 6-ML-thick sample. Equation (9) (serial connections) is not applicable for samples with average thickness less than about 1 ML that cannot form continuous paths in this simple model.

The results of the numerical calculations of Eq. (8) with δd from Fig. 5 are shown in Fig. 6. $k_F = 1.6062 \text{ \AA}^{-1}$ is obtained by fitting the energy dependence $E = \hbar^2 k^2 / (2m^*)$ to the experimental data of Fig. 11 in Ref. 21. The mean free path l of electrons was taken to be 20 \AA . Similar to the experimental data the plot shows a superposition of 1- and 2-ML oscillations. Note the 3-ML difference in thickness between the larger maxima at 12 and 15 ML. Close inspection of the experimental data in Fig. 3 shows such a difference in the same region.

The de Broglie wavelength λ_F and the thickness of separate islands nd_0 are in general incommensurate, so that the matching condition $m\lambda_F/2 = nd_0$ (QSE condition) will occur only within certain thickness ranges. For $\lambda_F/2 = \pi/k_F = 1.9559 \text{ \AA}$ and $d_0 = 2.86 \text{ \AA}$ this condition is well fulfilled for $n = 13$ ($nd_0 = 37.18 \text{ \AA}$) and $m = 19$ ($m\lambda_F/2 = 37.16 \text{ \AA}$) and approximately for $n = 2$, $m = 3$ and multiples of these pairs. However, $n = 13$ and $m = 19$ is just in the region of the mismatch both in the experimental data and in the calculated curves of Fig. 6. This mismatch can be explained as follows. A sudden decrease of the conductivity is expected when the thickness d crosses the value $m\lambda_F/2$ due to the sawtoothlike shape of the function $\sigma_{xx}(d)$ (if d is changing continuously). This shape describes the conductivity contribution of the regions with thickness nd_0 whose fractional coverage is $(\Theta_n - \Theta_{n+1})$. As can be seen in Fig. 5 the maxima of $(\Theta_n - \Theta_{n+1})$ and also the minima of the $(\delta d)^2$ vs d dependence are shifted about 0.2 ML when the growth front consists of 2 or 3 ML. This shifts the matching region to approximately 6 ML ($6d_0 = 17.16 \text{ \AA}$) with $m = 9$ ($9\lambda_F/2 = 17.60 \text{ \AA}$) and the mismatch region corresponding to about 11–14 ML.

IV. DISCUSSION AND SUMMARY

We have shown that ultrathin films of Pb and In-Pb alloys can grow on a Si(111)-(6×6)Au substrate at about 110 K in a quasi-monolayer-by-monolayer fashion. This was confirmed experimentally by RHEED specular beam intensity oscillations and by the appearance of CSE fine structure in the electrical resistivity. In comparison with theory it has to be kept in mind that Trivedi and Ashcroft⁹ have calculated the conductivity of ultrathin metallic films for 0 K temperature (when no energy-level smearing occurs) and for a uniform impurity distribution in the whole film while the experiment was performed at about 110 K, possibly with an impurity gradient at the film-substrate interface. Also the nature of the surface roughness distribution can strongly modify the $\sigma(d)$ dependence. Figure 3 of the second paper by Fishman and Calecki¹⁰ clearly shows that in the thickness range in which d is comparable to λ_F the surface conductivity σ_s decreases over 2 orders of magnitude when the autocorrelation length ξ decreases from 35 to 5 Å. This changes the slope of the σ vs d dependence for ultrathin films when surface roughness scattering is dominant. Figures 2 and 3 of Ref. 10 show also another important result: the positions and the shape of the QSE-induced maxima of $\sigma_s(d)$ depend on both the autocorrelation length ξ and on the shape of the autocorrelation function. Therefore, a change of ξ and/or the autocorrelation function during film growth can influence the QSE periodicity and/or the shape of QSE fine structure. This effect can be important in the analysis of the early stages of the film growth in which surface scattering is dominating volume scattering.

The $\sigma(d)$ dependence of both Pb and Pb-In films followed the law $\sigma \propto d$. In terms of the QSE theories^{7,10} this means that the correlation length of the surface roughness ξ is larger than k_F^{-1} or is increasing significantly with thickness.

The discrete nature of the resistivity oscillations with 1- and 2-ML period is a consequence of the quasi-monolayer-by-monolayer growth mode of Pb-In films, as observed also in the RHEED intensity measurements. A film-growth model with continuously changing thickness d gives maxima of σ every $\pi/k_F = 0.6839d_0$, which is not observed in experiment. We note that the conductivity calculated according to Eqs. (8) and (9) without inclusion of the small-scale roughness ($\delta d = 0$) gives the 2-ML-period oscillations, but the 1-ML-period oscillations are absent.

Although the oscillations with a period of 1 ML may be regarded as a CSE effect caused by a periodic variation of the specular parameter p in the Fuchs-Sondheimer theory, it must rather be considered as a quantum-mechanical phenomenon as clearly described in the theory of Trivedi and Ashcroft.⁹ This becomes evident upon a closer inspection of the ρ_∞ and $(1-p)l$ values shown in Table I. For a spherical Fermi surface the mean free path l is related to the resistivity $\rho_\infty = 1/\sigma$ via

$$l = \frac{3\pi^2\hbar}{e^2} \frac{1}{k_F^2\rho_\infty}. \quad (10)$$

This is true both for the Drude theory and the

quantum-mechanical theory which can be seen from Eq. (2) for $d \rightarrow \infty$. With $k_F = 1.606 \text{ \AA}^{-1}$ one obtains $l = 40, 37, \text{ and } 24.5 \text{ \AA}$ for samples *A, B, and C*, respectively, i.e., values which are considerably smaller than the corresponding $(1-p)l$ values in Table I. As $p \geq 0$ in the Fuchs-Sondheimer theory, the two sets of values are obviously inconsistent. The inconsistency can be explained by the quantum-mechanical theory in terms of a small coherence length of the roughness and/or a large roughness which can lead to negative p values in the classical theory.⁶ In addition, the classical theory cannot explain the oscillations with a period of 2 ML in regions in which the matching condition $nd_0 = m\lambda_F/2$ is approximately fulfilled. Thus, the Fuchs-Sondheimer theory leads to a pseudounderstanding of the conductivity of ultrathin metal films, i.e., of films in which the thickness d is comparable with the Fermi wavelength λ_F .

The same conclusion applies to our previous work in which for pure Pb films deposited at 95 K on the same substrate $\rho_\infty = 8.3 \mu\Omega \text{ cm}$ —corresponding to $l = 57 \text{ \AA}$ —and $(1-p)l = 90 \text{ \AA}$ was obtained (Table I in Ref. 13). The larger l value in that study is probably due to the lower temperature and small differences in film structure. It should be noted that the decrease of l from 40 Å to 24.5 Å with increasing In concentration agrees qualitatively with what one would expect for impurity scattering and that the value $l = 24.5 \text{ \AA}$ for 25 at.% In is close to the value 20 Å needed in the σ calculations with Eqs. (2) and (8), together with $A = 0.925$, in order to obtain best agreement between theory (Fig. 6) and experiment (Fig. 2) for the 25 at.% In film.

We conclude that QSE conductivity oscillations are a common phenomenon in sufficiently perfect ultrathin metal films with partially filled valence band in the direction of the size quantization. Contrary to previous indications we predict that the observation of the QSE in the

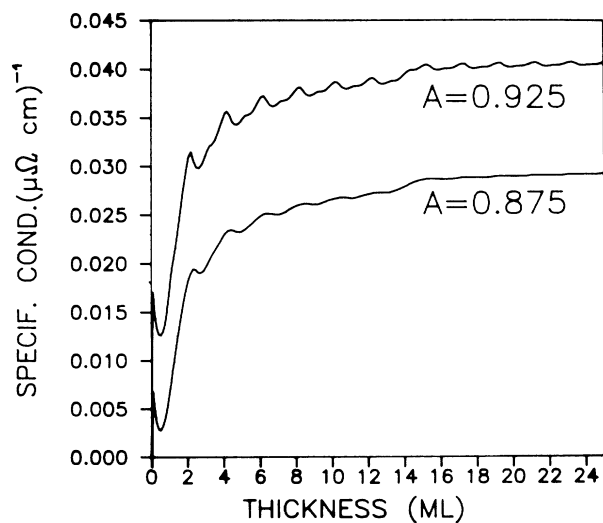


FIG. 6. The specific conductivity of a thin Pb film calculated with Eq. (8) using the $(\delta d)^2$ data shown in Fig. 5. The curve with $A = 0.875$ is shifted by $-0.01 (\mu\Omega \text{ cm})^{-1}$ for better viewing.

conductivity of ultrathin metal films is more probably in materials with small λ_F because the matching of the de Broglie wavelength with thickness within a limited thickness range $d \leq l$ is easier.

The experimental results and the quantitative analysis within the framework of the QSE theory stress the importance of the growth mode of the film and the strong influence of the surface condition on the appearance of QSE fine structures. From this point of view previous results in which a continuous variation of the thickness d was assumed²³ appear rather questionable. Also, the growth model with a period of 2 ML introduced to explain the 2-ML periodicity observed in He atomic beam scattering during the growth of ultrathin Pb films²⁴ is in contradiction to our results. More likely, these oscillations are due to the theoretically predicted²⁵ QSE oscillations of the spatial distribution of the electron density on the surface with which the He atoms interact.

Theoretical studies⁹ showed that the dominant source of resistivity oscillations is in the matrix element of the transition probability and not in the density of states. This work confirms this prediction experimentally. The

less perfect samples with smaller mean free path l (samples B and C in Figs. 2 and 4) show an enhancement of the QSE fine structures.

In conclusion, we have found a method to influence both CSE and QSE phenomena by using codeposition of Pb and In. Using this method, we have shown that the influence of the surface on the resistivity of ultrathin metal films can be described qualitatively but inconsistently within the framework of classical theories but that a quantitative and self-consistent description requires a quantum-mechanical treatment as given in Ref. 9, taking into account the nonmonotonic thickness changes on a microscopic level and the thickness dependence of the roughness correlations.

ACKNOWLEDGMENTS

This work was supported by the Volkswagen Foundation (Hannover, Germany), by the Deutsche Forschungsgemeinschaft, and by Grant No. 2-0382-91-01 of the Polish Committee of Scientific Research.

-
- ¹K. Fuchs, Proc. Cambridge Philos. Soc. **34**, 100 (1938); E. H. Sondheimer, Adv. Phys. **1**, 1 (1952).
²C. R. Tellier and A. J. Tessier, *Size Effects in Thin Films* (Elsevier, Amsterdam, 1982).
³V. B. Sandomirski, Zh. Exp. Teor. Fiz. **52**, 158 (1967) [Sov. Phys. JETP **25**, 101, (1967)].
⁴R. Kubo, J. Phys. Soc. Jpn. **12**, 579 (1967).
⁵G. Govindaray and V. Devanathan, Phys. Rev. B **34**, 5904 (1986).
⁶K. M. Leung, Phys. Rev. B **30**, 647 (1984).
⁷Z. Tešanović and M. V. Jarić, Phys. Rev. Lett. **57**, 2760 (1986).
⁸J. Y. Duboz, P. A. Badoz, and E. Rosencher, Appl. Phys. Lett. **53**, 788 (1988).
⁹N. Trivedi and N. W. Ashcroft, Phys. Rev. B **38**, 12 298 (1988).
¹⁰G. Fishman and D. Calecki, Phys. Rev. Lett. **62**, 1302 (1989); Phys. Rev. B **43**, 11 581 (1991).
¹¹G. Fischer and H. Hoffman, Z. Phys. B **39**, 287 (1980); G. Fischer, H. Hoffman, and J. Vancea, Phys. Rev. B **22**, 6065 (1980).
¹²D. Schumacher and D. Stark, Surf. Sci. **123**, 384 (1982).
¹³M. Jałochowski and E. Bauer, Phys. Rev. B **38**, 5272 (1988).
¹⁴M. Jałochowski and E. Bauer, J. Appl. Phys. **63**, 4501 (1988).
¹⁵P. I. Cohen, G. S. Petrich, P. R. Pukite, G. J. Whaley, and A. S. Arrott, Surf. Sci. **216**, 222 (1989).
¹⁶J. J. Harris, B. A. Joyce, and P. J. Dobson, Surf. Sci. **103**, L90 (1981); **108**, L444 (1981).
¹⁷S. T. Purcell, B. Heinrich, and A. S. Arrott, Phys. Rev. B **35**, 6458 (1987).
¹⁸C. Koziol, G. Lilienkamp, and E. Bauer, Appl. Phys. Lett. **51**, 901 (1987).
¹⁹Max Hansen, *Constitution of Binary Alloys* (McGraw-Hill, New York, 1958), p. 854.
²⁰M. Jałochowski and E. Bauer, Phys. Rev. B **37**, 8622 (1988).
²¹R. C. Jaklevic and J. Lambe, Phys. Rev. B **12**, 4146 (1975). m^* is calculated from the value $V_g = 1.7 \times 10^8$ cm/s in Table I.
²²M. Horn, V. Götter, and M. Henzler, in *Reflection High-Energy Electron Diffraction and Reflection Electron Imaging of Surfaces*, edited by P. K. Larsen and P. J. Dobson (Plenum, New York, 1988), p. 463.
²³H. Hoffman, *Festkörperprobleme*, edited by P. Grosse (Vieweg, Braunschweig, 1982), p. 255.
²⁴B. J. Hinch, C. Koziol, J. P. Toennies, and G. Zhang, Europhys. Lett. **10**, 341 (1989); Vacuum **42**, 309 (1991).
²⁵F. K. Schulte, Surf. Sci. **55**, 427 (1976).